I. J. Computer Network and Information Security, **2024, 4, 31-51**
Published Online on August 8, 2024 by MECS Press (http://www.mecs-press.org/)
DOI: 10.5815/ijcnis.2024.04.03

Passive Antenna Arrays in UAV Communication Systems

Olga Shcherbyna*
Department of Electronics, Robotics, Monitoring and IoT Technologies, National Aviation University, Kyiv, 03058, Ukraine
E-mail: shcherbyna_ol@nau.edu.ua
*Corresponding author

Oleksandr Zadorozhnyi
Department of Electronics, Robotics, Monitoring and IoT Technologies, National Aviation University, Kyiv, 03058, Ukraine
E-mail: olserza@gmail.com

Olexii Stetsyshin
Department of Electronics, Robotics, Monitoring and IoT Technologies, National Aviation University, Kyiv, 03058, Ukraine
E-mail: 4592819@stud.nau.edu.ua

Received: 06 February 2023; Revised: 16 May 2023; Accepted: 17 July 2023; Published: 08 August 2024

Abstract: This article explores the design, modeling, and experimental validation of passive antenna arrays (AAs) tailored for unmanned aerial vehicle (UAV) communication systems. Focusing on the technical composition and functionalities of various types of passive antenna arrays, the study delves into different antenna elements that comprise these arrays, discussing their integration into comprehensive systems. Through rigorous modeling aimed at predicting performance in diverse operational conditions and backed by experimental studies, the paper provides practical insights for the development and optimization of AAs. These passive systems leverage the collective strength of multiple antennas to form directed beams, enhancing signal clarity and reducing interference, thereby supporting robust communication links essential for UAV operations.

Index Terms: Unmanned Aerial Vehicles, Passive Antenna Arrays, Ground and Airborne Control Segment, Dipole Antennas, Collinear Antennas, Planar Antenna Arrays, Log-Periodic Antenna, Yagi-Uda Antenna.

1. Introduction

Unmanned aerial vehicle (UAV) is a device capable of flying remotely with control or autonomously following a preset course, transmitting or storing information according to its mission. There is no generalized system for classifying UAVs. They can vary in weight and size, ranging from devices just a few centimeters in size to aircraft with wingspans of up to ten meters. Among the numerous characteristics of UAVs, notable ones include operational altitude, range, and general performance features. There are several main classifications of UAVs by functionality: reconnaissance, combat, logistics, research, civilian, and commercial. Reconnaissance and combat UAVs are used on the battlefield for high-risk reconnaissance missions. Logistic UAVs are used for cargo logistics operations. Research drones are used for various scientific projects and to determine the further development of UAV technologies.

UAV development and production are continuously evolving. Currently, the defense sector is and likely will continue to be the main market for UAVs. However, there is also ongoing expansion in the civilian and commercial use of UAVs. Manufacturers are increasingly focusing on developing aircraft for use in border missions, humanitarian aid, search and rescue, scientific research, meteorology, fire monitoring, agriculture, infrastructure inspection, police surveillance, cargo delivery, and signal transmission.

An UAV system is not only the aircraft itself but a complex system that maintains communication with a ground control station. This requires a large number of electronic devices for recording, receiving, and transmitting data, as well as for avionics functions. They have become integral across various domains including military real-time surveillance, using not only optical but also radar means [1, 2], commercial logistics, and environmental monitoring [3]. As UAVs

operate in complex and dynamic environments, the demand for sophisticated communication systems to ensure reliable data exchange, control [4, 5], precise navigation [6], trajectory correction [7], and surveillance [8] has grown exponentially.

The antenna is a key component of any of mentioned telecommunication branches. Thus, antennas are one of the most critical electronic devices in any UAV system, as they enable the vehicle to transmit and receive information from other systems, including the ground segment of control. Exactly antenna largely determines the configuration and often appearance of the entire system. Passive antenna arrays stand out in this landscape, offering significant improvements in signal reception and transmission without the dependency on external power sources. Passive antenna arrays have become essential in this context, providing robust improvements in signal reception and transmission, crucial for UAVs operating in challenging environments. These arrays, utilizing the collaborative function of multiple antennas, direct beams effectively to enhance signal clarity and reduce interference, vital for reliable communication. Such antenna arrays leverage the collective strength of multiple antennas to form directed beams, enhancing signal strength and reducing interference, which is crucial for maintaining robust communication links. This technology is especially effective in supporting multiple-input multiple-output (MIMO) systems [10], which are essential for enhancing data throughput and the reliability of UAV communications by enabling multiple simultaneous transmissions over the same channel.

Moreover, the potential integration of passive antenna arrays with ultra-wideband (UWB) technology [10, 11] opens new possibilities for UAV applications. UWB is prized for its high resolution and precision, making it ideal for applications requiring accurate navigation and real-time surveillance. The spatial diversity offered by antenna arrays can significantly boost UWB device performance, enhancing their capability in secure, high-speed data transmission and precise localization tasks [12].

Antennas used both for onboard systems and in mobile control systems of UAVs need to be low-profile and compact, have a strong, simple, and lightweight design, and be easily mountable on various surface shapes. The radiation parameters of antenna systems depending on the purpose of the system may have a sufficiently wide nomenclature.

Typically, both the airborne and ground segments of the remote-control system of UAVs include dipole omnidirectional antennas with linear polarization or simple antennas with circular polarization (for example, cloverleaf or Pagoda antennas). The advantage of this approach is broad angular coverage, which is crucial given the UAVs' continual change in location. However, these antennas have a relatively low gain (about 2 dBi), which may limit communication over long distances. Omnidirectional antennas are also more vulnerable to electronic warfare (EW) interference. To solve this problem, it is appropriate to use either directional antennas or antenna arrays (AA) on the ground control segment. For example, spiral, parabolic, horn antennas, Yagi-Uda antennas, log-periodic antennas, linear or flat AA can be used.

Using AAs allows for the tasks of forming specifically shaped radiation patterns, controlling the shape of the radiation pattern, orientation control in space, scanning space, and increasing radiation power, among others.

The use of such passive AAs allows for the creation of radiation patterns with narrow main lobes, specially shaped radiation patterns, increased radiation power, as well as applying enhanced design technology. Passive AAs enable the use of a combination of weakly directional radiating elements to create the necessary field distribution in space, apply aperture control for radiation pattern formation quality, and perform tuning with relative ease, simultaneously forming several radiation patterns. These positive properties of AAs with static amplitude-phase distribution have ensured their widespread use in radio engineering and telecommunications.

Numerous works are dedicated to the principles of design, modeling, and research of AAs of various constructions. In the overview part of this study, several works are considered that are closely related to our objectives focusing on such characteristics as the half-power beamwidth (HPBW) and gain factor. In these studies, antennas are considered for various segments of radio electronics and telecommunications, however, such designs can easily be adapted for UAV communications purposes.

The paper [13] proposed a simple and compact Yagi-Uda antenna on Rogers RO4003 substrate for multi-band radar applications. The prototype operates in three different frequency bands, namely 1.9, 2.5 and 3.5 GHz with gains of 6.29, 4.63 and 6.77 dBi, respectively. The goal of the research work [14] is to develop a planar compact Yagi-Uda antenna for 2.4 GHz WLAN applications. This document discusses methods for increasing antenna gain. The proposed antenna is designed and manufactured on FR-4 substrate. The maximum antenna gain is 4.34 dBi. The above articles do not provide the exact HPBW values that the prototypes showed. But, analyzing the indicated radiation patterns, we can assume that these values are in the range of 120-130 deg. in the H-plane and 60-70 deg. in the E-plane, which is typical for Yagi-Uda antennas.

The combination of helical elements of different lengths makes it possible to implement a dual-band helical antenna, the study of which is described in the work [15]. This article describes the construction of twelve-element slot helical antenna with right-handed circular polarization for frequencies 1.227 GHz and 1.575 GHz (GPS L1 and L2 bands). For these frequencies, gains of 4.44 and 3.87 dBi were obtained at HPBW of 96 deg. and 122 deg., respectively. The principles of constructing wire and microstrip four-element helical antennas were given in [16, 17]. Simulations were carried out of two versions of the wired and one version of the printed helical quadrifilar antenna for BD3 band of the Chinese navigation satellite system BeiDou (1268.52 ± 12 MHz). Simulation and experimental study showed voltage standing wave ratio (VSWR) of less than 1.5 in the operating frequency range with the gain of about 3 dBi at HPBW 90 deg.

In the article [18], a comparison of the matching and radiation parameters of broadband microstrip log-periodic antennas (LPAs) in the frequency band 2-5 GHz using dielectric substrates with different characteristics was made. As a

result of modeling and experimental study of three samples, the gain of more than 6 dBi was obtained over the entire frequency band. But it was emphasized that to improve the quality of microstrip LPAs and the stability of main characteristics at frequencies above 3.5 GHz, it is advisable to use specialized microwave substrates for manufacturing (for example, Roger RO4003C). As a result of the research in [19], an LPA design for WLAN/LTE/UWB applications was obtained, manufactured on an FR4 substrate with dielectric constant of 4.3. The measurement results showed that the proposed antenna has wide bandwidth from 1.4 to 12 GHz, providing the average gain of 4.51 dBi.

The article [20] presents fairly successful design of the 12-element slot AA, which, when positioned vertically, can provide the HPBW in the meridional plane of about 7 deg. with the gain of 17 dBi.

The work [21] is devoted to the development and research of compact coaxial collinear AA for mobile satellite communications at the frequency of 4.2 GHz. The AA consists of 10 elements and provides the gain of about 4.5 dBi in the directions of 20 and 240 deg., which is suitable for use in satellite communication systems.

The paper [22] presents the 2 x 2 microstrip AA design with rectangular patch elements for the frequency of 3.8 GHz, having the HPBW of 33 deg. and the gain of 13.2 dBi. The compact two-element AA design with vertical polarization for portable UAV remote control is considered in [23]. This AA operates at the frequency of 2.4 GHz. To increase the radiation efficiency, patch elements with air cavities were used. When modeling and studying this AA, the gain of 9.14 dBi was achieved at the HPBW of 60 deg. in the E-plane and 65 deg. in the H-plane. The study [24] presents the design and implementation of four linear AAs consisting of microstrip rectangular antennas. Linear AAs operate in the frequency range from 2.62 to 2.69 GHz and provide cosecant quadratic radiation pattern in the E-plane and the HPBW of about 90 deg. in the H-plane with the maximum gain of 11.1 dB to 12.2 dB in the operating frequency band.

Unfortunately, in all the works discussed above, there is no indication of the features that arise during the modeling, manufacturing and operation of the developed AA structures. Only the final results of the study are indicated there. Although, according to the experience of the authors of this work, as a result of the development of any type of antenna, nuances arise, taking into account which significantly simplifies the work and improves the final result. It would be very useful to have practical guidelines to help researchers and developers of antennas and antenna systems optimize performance and achieve their goals.

This article focuses primarily on the technical composition and capabilities of various types of passive AAs suitable for UAV systems applications. We delve into the different types of antenna elements that compose these arrays and discuss their design and integration into comprehensive systems. Detailed attention is given to the modeling of these arrays to predict their performance in diverse operational conditions and to the experimental studies that validate these models. The aim is to provide a thorough exploration of passive antenna arrays, offering practical recommendations and insights that can aid in their development and optimization.

The study involves the modeling and research of several types of passive AAs with static amplitude-phase distribution. These samples relate to AAs that are most convenient for use in UAV communication systems, meeting the requirements for compactness, simplicity, reliability, and having good radiation and matching characteristics.

Through this article, we aim to convey to researchers and practitioners our experience, research results and knowledge necessary to improve the design and functionality of passive AAs to increasing their effectiveness in UAV communications systems. By focusing on the arrays' structural and functional aspects, this article contributes to a deeper understanding of their potential and the technical nuances involved in their development using different antenna elements.

In Section 2, an overview of the main principles of designing passive AAs of two types will be conducted: equidistant in-phase equal-amplitude and non-equidistant unequal-amplitude. Section 3 is dedicated to the development process, modeling, and experimental research of six samples of AAs of different types: microstrip flat AA 4x2, two samples of Franklin antennas, coaxial collinear antenna, microstrip Yagi-Uda antenna, and microstrip log-periodic antenna.

2. Principles of Passive Antenna Array Construction

Structurally, passive AA can generally be divided according to the following criteria:

- according to the order of placement of AA elements: linear, flat and volumetric; equidistant or non-equidistant;
- according to the principle of feeding AA elements: equal-amplitude and unequal-amplitude; in-phase and phase-shifted.

Let us briefly consider the theoretical principles of constructing different types of AA that will be studied in this work.

2.1. Equidistant In-phase Antenna Array

Fig. 1 shows the linear equidistant in-phase AA with static amplitude-phase distribution.

The field intensity at the observation points from such AA, consisting of the set of n emitters, is equal to:

$$\dot{E} = E_{\max} F(\theta,\varphi) \frac{\sin\left[\frac{nkd\cos\theta}{2}\right]}{\sin\left[\frac{kd\cos\theta}{2}\right]} e^{ikr},$$

where $E_{\max}$ is amplitude multiplier, the value of which depends on the power supply intensity of the emitters, their design and distance to the observation point; $F(\theta,\varphi)$ is normalized radiation pattern (RP) of identical emitters; $F_s(\theta) = \sin\left[\frac{nkd\cos\theta}{2}\right] \Big/ \sin\left[\frac{kd\cos\theta}{2}\right]$ is system multiplier; r is the distance from the AA center to the observation point; d is the distance between two adjacent AA emitters; θ is meridional angle; $k = 2\pi/\lambda$ is wave number.

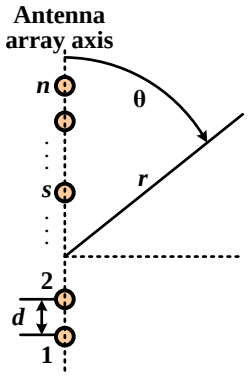

Fig.1. The emitters system that are discretely located along the system axis

That is, AA RP radiation pattern is the product of two factors:

$$f(\theta,\varphi) = F(\theta,\varphi) F_s(\theta),$$

the first of which describes the guiding properties of individual emitters, and the second (system multiplier) takes into account the fields interference of all system emitters.

Provided that $kd < 2\pi$, AA RP will have one main lobe. The direction of the main maximum can be defined as $\cos\theta_{\max} = 0$. Consequently, the maximum radiation direction of an in-phase linear system coincides with the perpendicular to the emitters location line.

Directions of zeros and side lobes of the RP of the linear equidistant in-phase AA are defined as:

$$\cos\theta_{0p} = \frac{2p\pi}{nkd}, \quad p = \pm1, \pm2, \pm3, \ldots;$$

$$\cos\theta_{mp} = \frac{(2p+1)\pi}{nkd}, \quad p = +1, \pm2, \pm3, \ldots,$$

where θ_{0p} is zero radiation direction of *p*-th order; θ_{mp} is the direction of the side lobe maximum of the *p*-th order.

Unidirectional radiation can be obtained using a reflector (screen). The reflector is placed at the distance (0.2–0.25) λ from the AA plane. For example, the directivity characteristic in the horizontal (azimuthal) plane, as follows from Fig. 2, is determined by the directional properties of individual AA elements (for example, symmetrical dipoles), the system multiplier and the reflector influence. According to the multiplication theorem, the directivity characteristic can be written as

$$f(\varphi) = F(\varphi) F_s(\varphi) f_r(\varphi),$$

where $F(\varphi)$ is the directivity characteristic of individual element in the azimuthal plane; $F_s(\varphi) = \sin\left(\frac{1}{2} m\pi \sin\varphi\right) \Big/ m\sin\left(\frac{1}{2}\pi\sin\varphi\right)$ is the system multiplier for the distance between AA elements $d = 0.5\lambda$ and

the number of elements m; $F_r(\varphi) = \cos\left(\frac{\pi}{4}(1-\cos\varphi)\right)$ is the multiplier that takes into account the reflector influence, which is powered by the current shifted in phase by 90° relative to the antenna current and located at the distance d_r = 0.25λ; φ is azimuthal angle.

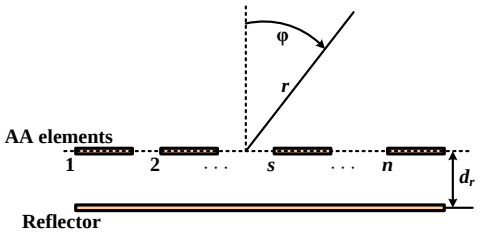

Fig.2. AA with the reflector in the azimuthal plane

Any omnidirectional or directional antennas can be used as elements of linear or flat equidistant AA. For example, half-wave symmetrical and asymmetrical dipoles with different arm designs are most often used (Fig. 3).

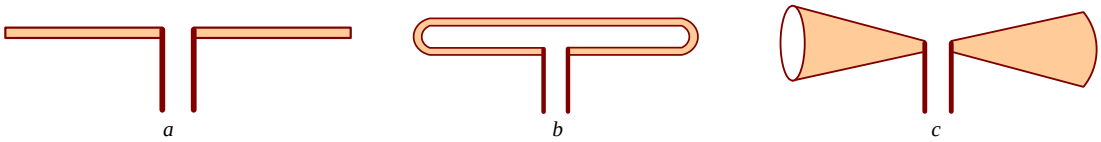

Fig.3. Examples of arms designs of symmetrical dipole: *a* – classic rectilinear; *b* – folded dipole; *c* – biconical dipole

As elements of microstrip equidistant in-phase AA, many researchers choose simple rectangular patch element (Fig.4) with different power supply methods, the construction of which is described in detail in many scientific works [21-25].

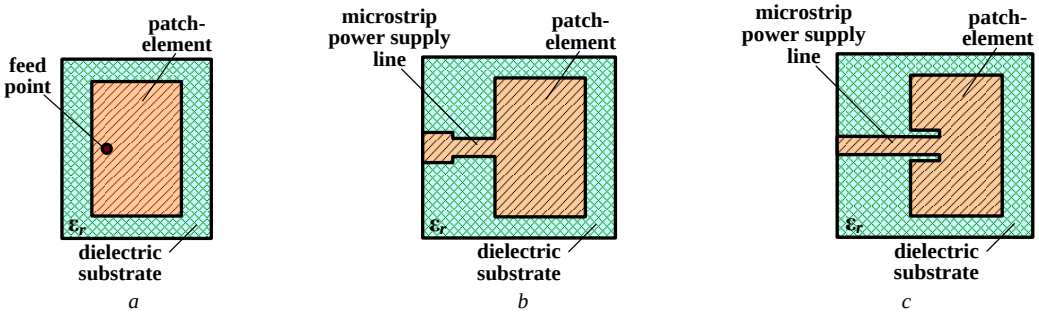

Fig.4. Examples of connecting microstrip patch antennas: *a* – power supply using coaxial probe; *b* – power supply using microstrip line with quarter-wave matching transformer; *c* – power supply using microstrip line with an insert

2.2. Non-equidistant Unequal-amplitude Antenna Array

The most famous examples of non-equidistant unequal-amplitude AA are the Yagi-Uda antenna (director antenna, wave channel antenna) and the log-periodic antenna.

The Yagi-Uda antenna design is shown schematically in Fig. 5. The dipoles axes are parallel to each other, perpendicular to the antenna axis and are in the same plane. Of the entire set of dipoles, only one is active (*A*). The remaining dipoles (the reflector *R* and directors *D*) are passive and are excited by the field of the active dipole.

The phase relationships of the re-emission fields of passive dipoles are selected in such a way that the resulting field of the entire antenna has the highest intensity in the direction of the antenna axis. In this case, the maximum radiation is directed towards the directors.

The reflector *R* reduces the antenna radiation into the half-space located to the left of the reflector (Fig. 5). Since the field behind the reflector is significantly weakened, one dipole is sufficient to create unidirectional radiation from the antenna. To weaken the field in the left half-space, it is necessary that the waves emitted by dipole *R* be in antiphase with the waves of the dipole *A* when propagating into the left half-space and be in phase with the waves of the dipole *A* when propagating into the right half-space (towards the directors). This condition is satisfied if the reflector current is in phase ahead of the active vibrator current. This is achieved due to inductive nature of the reflector impedance. To do this, it is necessary to take the reflector length slightly longer than half wavelength. The active dipole operates at its own wavelength ($2l$ = 0.5 λ), so the reflector length is taken to be (5...15) % greater than the active dipole length. The distance between the reflector and the active dipole is in the range (0.1...0.25) λ.

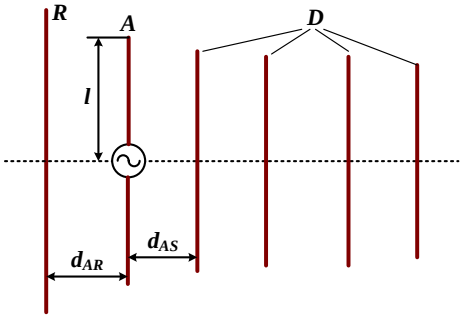

Fig.5. Yagi-Uda antenna

The directors are placed in the direction of radio waves propagation and contribute to electromagnetic energy concentration. To ensure maximum intensity in the antenna axis direction, the director's radiation field must be out of phase with the active dipole field. This is achieved by the phase lag of the currents in the directors. To do this, their impedance must be capacitive nature. To obtain the capacitive nature of the director's impedance, their length is chosen to be (5...15) % less than the active vibrator length. The distances between the active vibrator and the first director, as well as between the directors, are selected in the range from 0.1 to 0.35 λ.

The calculation of the Yagi-Uda antenna is quite complicated. As a result of solving the equations system, the current values in the antenna elements is obtained, which makes it possible to calculate the system multiplier:

$$f_s(\theta) = \frac{I_R}{I_A} e^{-ikd_{AR}\cos\theta} + 1 + \sum_{s=1}^{n} \frac{I_S}{I_A} e^{ikd_{AS}\cos\theta},$$

where I_R is reflector current, I_S is director current, I_A is active dipole current, d_{AR} is the distance between the reflector and the active dipole, d_{AS} is the distance between the active dipole and the s-th director, θ is the angle between the antenna axis and the direction to the observation point.

The input impedance of the Yagi-Uda antenna can be quite low due to the fact that the induced resistances of the passive dipoles are negative. Therefore, in the case of using half-wave symmetrical dipole as the active emitter, the input impedance is about 20-30 Ohms. If the active emitter is the folded dipole, then the input impedance is 120-180 Ohms. The Yagi-Uda antenna has a simple and durable design. Its disadvantage is its narrowband and configuration complexity.

An antenna with a logarithmic-periodic structure (***log-periodic antenna*** LPA) belongs to the class of ultra-wideband antennas. Its bandwidth ratio reaches values of more than 4. The directional coefficient of such antennas is relatively small and amounts to 10-11 dB, but the operating frequency band is quite large. Therefore, LPAs find a very wide range of applications.

The flat LPA has the form of linear AA of symmetrical dipoles, the length of which varies monotonically (Fig. 6). Dipoles are powered by a two-wire feeder. The lines connecting dipoles ends create the antenna angle α.

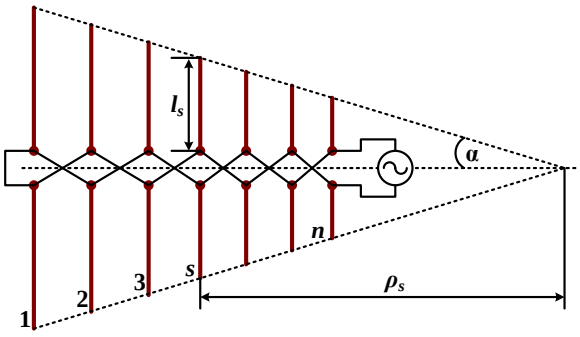

Fig.6. LPA design

Conditions for log-periodic structure:

- tangent of half antenna opening angle

$$\frac{l_1}{\rho_1} = \frac{l_2}{\rho_2} = \ldots = \frac{l_n}{\rho_n} = \mathrm{tg}\frac{\alpha}{2};$$

- relative diameter of the s-th dipole

$$\sigma = \frac{a_s}{\rho_s} = \text{const},$$

where a_s is the diameter of the s-th dipole;

- relative distance between adjacent dipoles

$$\tau = \frac{\rho_{s+1}}{\rho_i} = \text{const}.$$

The requirement to maintain a constant relative diameter of the dipole elements is not critical, therefore, in violation event, the antenna retains frequency independence. Therefore, dipoles can be made with the same cross-section. The first and third conditions must be satisfied with great accuracy. Only in this case the basic properties of the antenna are preserved.

The dipoles whose length is close to or equal to half wavelength have the small input impedance, in which the active component predominates. The currents in these dipoles will be significant and therefore the radiation intensity of electromagnetic waves compared to the waves intensity emitted by other dipoles is very high. The dipoles that intensely emit waves create the LPA's active zone. The LPA active zone is equivalent to the Yagi-Uda antenna consisting of three dipoles. As the wavelength changes, the active zone shifts along the LPA.

Due to the fact that the relative length of the active zone dipoles is unchanged, the antenna parameters for all resonant wavelengths are repeated. When designing an antenna, its constants α and τ are selected in such a way that changes in the antenna parameters do not exceed acceptable limits.

The resonant wavelength value of the s-th dipole is determined by the formula in terms of the resonant wavelength of the first dipole:

$$\ln \lambda_s = (s-1)\ln \tau + \ln \lambda_1.$$

Therefore, on logarithmic scale, the resonant wavelengths repeat at equal intervals ln τ. This circumstance determines the antenna name.

3. Modeling and Research of Antenna Arrays

The basic general principles of AA design were described in the previous section. This section discusses some practical features when constructing various AA designs that can improve the matching and radiation parameters of the antenna and which are recommended to be taken into account during modeling and manufacturing. All experimental samples of the developed AAs were studied using the vector network analyzer Lite VNA 64.

3.1. Microstrip Flat Antenna Array 4 x 2

To construct microstrip flat equidistant equal-amplitude in-phase AAs, any microstrip elements can be used. But most often, as noted above, researchers use simple rectangular patch emitters as AA elements (Fig. 4). The advantages of these emitters are the ease of calculation described, for example, in [25, 26], and the possibility of relatively simple implementation of the radiation pattern with the required beamwidth. But there are also disadvantages. For example, a relatively narrow operating frequency band, which is unacceptable for some applications. Therefore, there is a need to use other AA element designs that would expand the frequency band.

In addition to the rectangular microstrip element, depending on the tasks set by the designer, many other modifications of the shape of the AA microstrip elements are used, which can improve such AA characteristics as the gain, the HPBW, the operating frequency bandwidth, and more. For example, to construct the AA with linear polarization, microstrip symmetrical dipole elements with different arm shapes are often used (classical rectilinear, bowtie antenna, folded dipole antenna, etc.).

In this work, the microstrip folded dipole antenna powered by two-wire microstrip line was used as AA elements (Fig. 7).

The main advantages of the folded dipole compared to the classic straight open dipole are:

- The folded dipole provides significant increase in the resistance level, which simplifies the matching of the antenna with the power line.
- The folded dipole has flatter frequency response, allowing it to be used over wider frequency range.

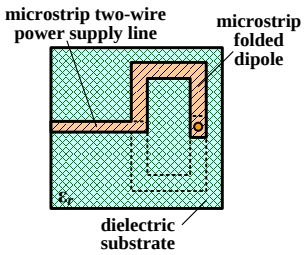

Fig.7. The microstrip folded dipole

To design the microstrip folded dipole as the AA element, it is necessary to know the parameters of a strip two-wire feeder (Fig. 8).

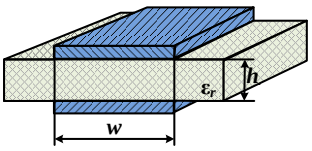

Fig.8. Two-wire strip feeder

The symmetrical strip two-wire feeder can be considered as two microstrip lines with a common shield. The characteristic impedance of such line is equal to twice the impedance of the single microstrip line, since the characteristic impedances of the microstrip line are connected in series. Therefore, for the calculation, expressions for the microstrip line can be used, in which it is necessary to double the characteristic impedance and reduce the substrate thickness *h* by half. As a result, from the expressions for the microstrip line impedance, a simplified formula for the width of the strip two-wire feeder is obtained:

$$w = \left(\frac{200\pi}{W_l \sqrt{\varepsilon_r}} - 1 \right) \left(\frac{h}{2} - \Delta_m \right),$$

where W_l is the characteristic impedance of the symmetrical microstrip feeder; Δ_m is metal thickness of the feeder strip; ε_r is relative permittivity of the substrate.

To optimize feeder dimensions, use the following inequality, provided that characteristic impedance of standard coaxial feeder $W_f = 50$ Ohm,

$$1.21 \le \frac{W_l}{W_f} \le 1.43 .$$

To build the microstrip flat AA 4 x 2 (Fig. 9), the elements of which are folded dipoles, the dielectric substrate Roger RO4030 was used with the following parameters:

- relative permittivity 3.38;
- dielectric loss tangent 0.0027;
- substrate thickness 0.813 mm.

Central operating frequency of the flat AA is 5.9 GHz.

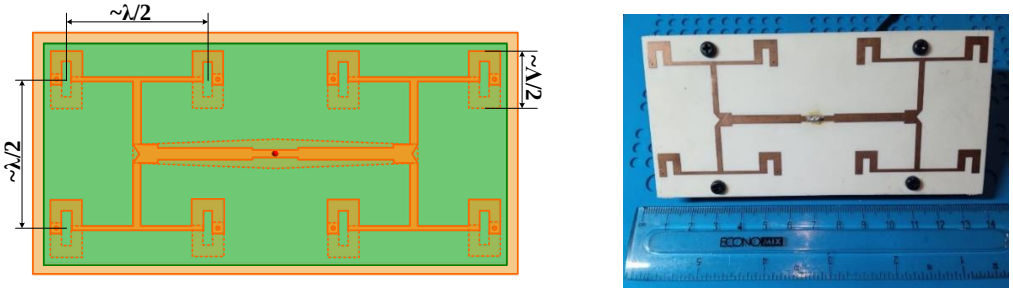

Fig.9. Microstrip flat AA 4 x 2

The main results of modeling and experimental research of the microstrip flat AA are presented in Fig. 10-14.

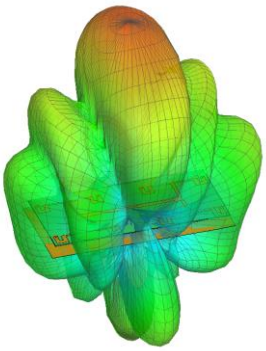

Fig.10. 3D radiation pattern of the microstrip flat AA 4 x 2

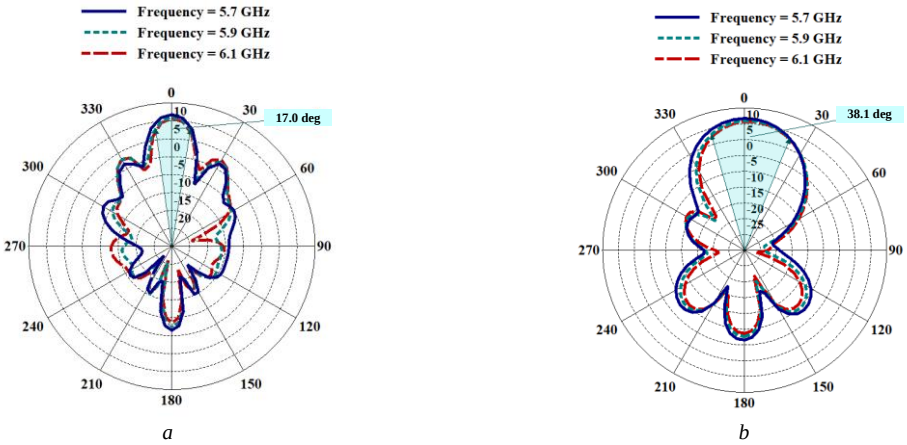

a *b*

Fig.11. Radiation patterns of the microstrip flat AA 4 x 2: *a* – in the plane φ = 0 deg.; *b* – in the plane φ = 90 deg

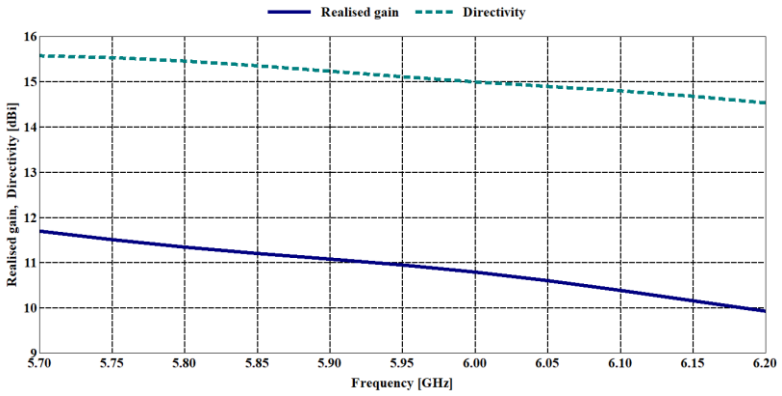

Fig.12. Dependences of the gain and the directivity of the microstrip AA 4 x 2 on the frequency

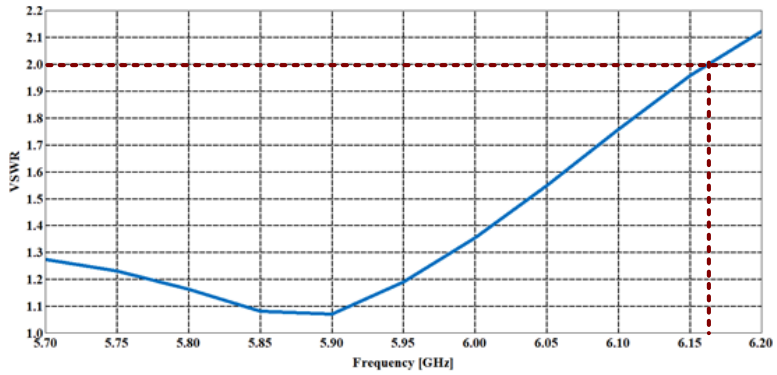

Fig.13. Dependence of the VSWR of the microstrip AA 4 x 2 on the frequency

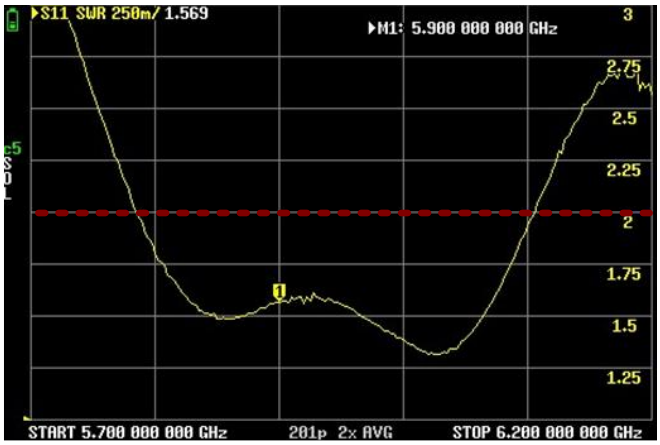

Fig.14. Measured dependence of the VSWR of the microstrip AA 4 x 2 on the frequency

The results of modeling the microstrip array 4 x 2, the elements of which are folded dipoles, showed the possibility of forming the radiation pattern with sufficiently narrow HPBW. When placing the antenna to work with vertical polarization, HPBW in the horizontal plane was 17 deg., in the vertical plane it was 38 deg. In this case, the level of the side lobes does not exceed –10 dB. The gain at the central operating frequency reaches 11 dBi. Experimental study showed that the operating frequency band of the antenna reaches 300 MHz with VSWR < 2 (5.8–6.1 GHz). The experimentally obtained frequency band is less than that obtained in the simulation. This is due to the inaccuracy of the production of the experimental sample. But the goal was achieved.

When modeling, manufacturing and studying the experimental sample, the following features were noted:

- to expand the operating frequency band, it is necessary not only to increase the radiating element width of the folded dipoles, but also to make small shift between the dipole arms on both sides of the substrate to reduce the quality factor;
- the distance between the AA elements at the first stages of design should be half the wavelength, but during the optimization process it definitely changes;
- this design requires careful calculation and maximum precision manufacturing; any inaccuracy of the experimental sample (dimensions of elements, distance to the screen, etc.) negates all expected results.

Flat in-phase arrays are quite widely used as antennas for the ground control segment of UAVs.

3.2. Collinear Antennas

A. Franklin Antenna

Collinear antennas belong to the class of linear in-phase AA, which are made of symmetrical dipoles. An example of collinear antenna design is Franklin antenna, created back in 1926. As can be seen from the design diagram (Fig. 15, *a*), the Franklin antenna consists of metal rods 0.5λ long and inductive coils connecting the rods.

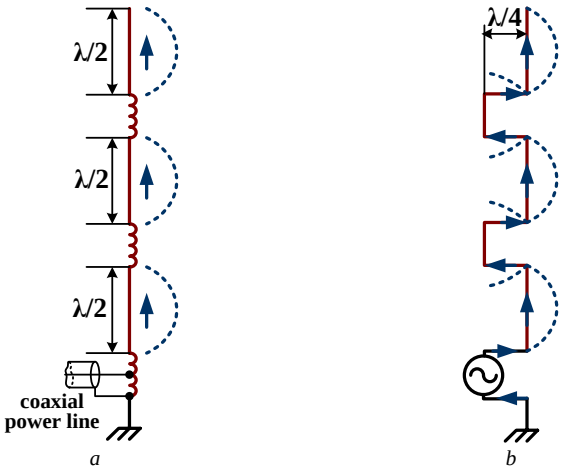

Fig.15. Franklin antenna

The generator powers the antenna using a coaxial cable connected to the antenna terminals through a matching device (autotransformer). With the correct choice of generator frequency, half wavelength is placed on the rods, and the

rods emit electromagnetic waves in the same way as half-wave symmetrical dipoles. The inductors absorb half the standing wavelength, which ensures in-phase excitation of the dipoles. The value of the inductances is chosen large enough so that half wavelength is also placed on the turns of the coils. The distributed capacitance between the turns should be accounted when calculating inductors.

The equivalent circuit of Franklin antenna is shown in Fig. 15, *b*. The inductors can be replaced with quarter-wave sections of short-circuited line. These conductors pick up half-waves of standing current in antiphase to the current in the dipoles. Consequently, the dipoles are powered by in-phase currents, and Franklin antenna can be considered as the in-phase AA. In the horizontal plane the collinear antenna is omnidirectional, and in the vertical plane the radiation is concentrated at small elevation angles. The beamwidth of the collinear antenna has slightly larger value than that of the equal-amplitude AA, since the greater the distance of the dipole from the antenna terminals, the smaller the current amplitude. The side lobes' level is reduced compared to the equal-amplitude AA, but the gain does not reach the similar values. In modern collinear antennas, inductors are used with a small number of elements.

The collinear antenna was studied for the frequency range 730–760 MHz. For construction it was used:

- copper wire with the diameter of 2.5 mm;
- N pin connector for crimping RG-213 cable.

During the study, it was decided to compare two methods for constructing the collinear antenna: using the inductor (Fig. 16) and using the quarter-wave stub (Fig. 17) for phasing currents in the antenna elements.

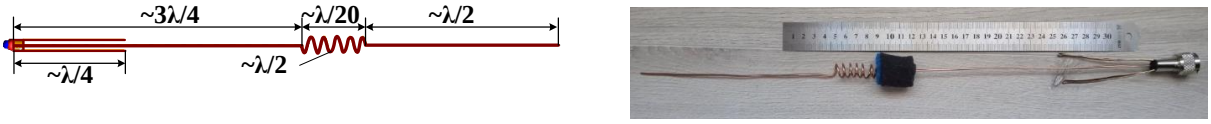

Fig.16. The collinear antenna with the inductor

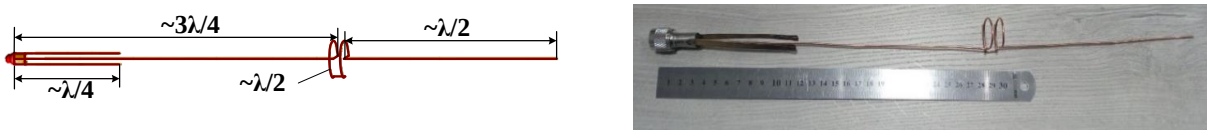

Fig.17. The collinear antenna with the quarter-wave stub

The main results of modeling and research of collinear wire antennas are presented in Fig. 18-22.

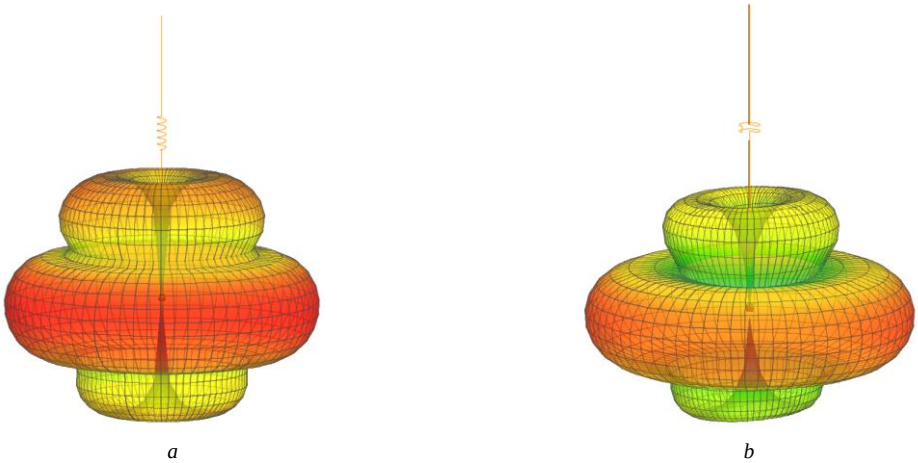

a *b*

Fig.18. 3D radiation patterns of the collinear antennas: *a* – with using the inductor; *b* – with using the quarter-wave stub

An experimental study of the samples showed that the operating frequency band of the collinear antennas reaches more than 200 MHz (710–820 MHz and 695–805 MHz, respectively) with VSWR < 2. The gain at the central frequency reaches 5 dBi at the HPBW value of about 30 deg.

The following features were noted during the modeling and study of the experimental samples:

- increasing the number of half-waves radiating elements does not significantly increase the gain (with the addition of one more element, the gain increased to 6 dB), so in most cases there is no point in increasing the collinear antenna length;
- the side lobes level when phasing AA elements using the quarter-wave stub is less than when using the inductor

(–9 dB and –6 dB, respectively);

- the manufacture of the collinear antenna with the inductor showed greater degree of repeatability, greater simplicity and manufacturability of the process than the second sample.

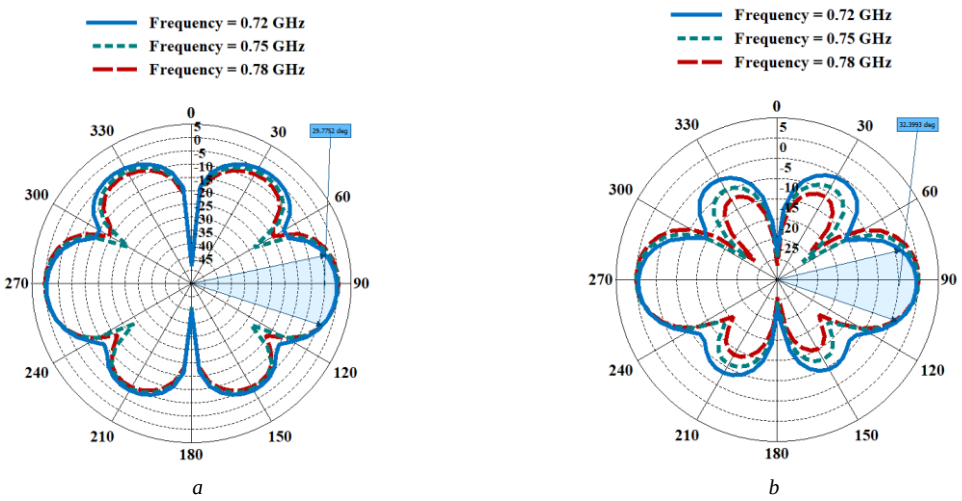

a *b*

Fig.19. Radiation patterns of the collinear antennas in the *E*-plane: *a* – with using the inductor; *b* – with using the quarter-wave stub

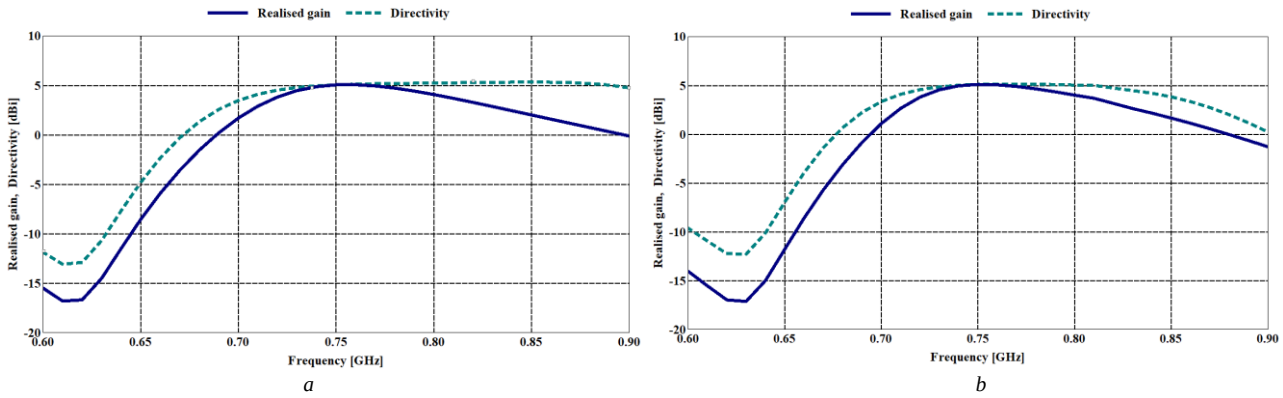

a *b*

Fig.20. Dependences of the gain and the directivity of the collinear antennas on the frequency: *a* – with using the inductor; *b* – with using the quarter-wave stub

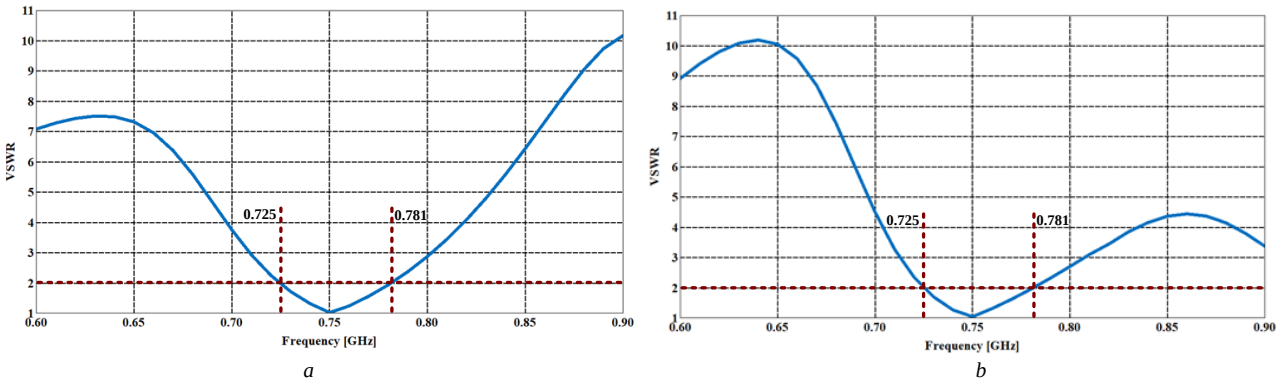

a *b*

Fig.21. Dependences of the VSWR of the collinear antennas on the frequency: *a* – with using the inductor; *b* – with using the quarter-wave stub

B. Coaxial Collinear Antenna

More technologically advanced design compared to wired collinear antennas are collinear antennas made from sections of coaxial wire (Fig. 23, *a*). Each of the cable segments is the half-wave dipole. Fig. 23, *b* shows longitudinal section of the coaxial collinear antenna. From the above diagram it can be seen that the segments are connected crosswise, which ensures that the currents on the outer surface of the coaxial rods are in-phase, provided that each segment contains half wavelength. Common-mode currents also flow on the central conductors of the coax.

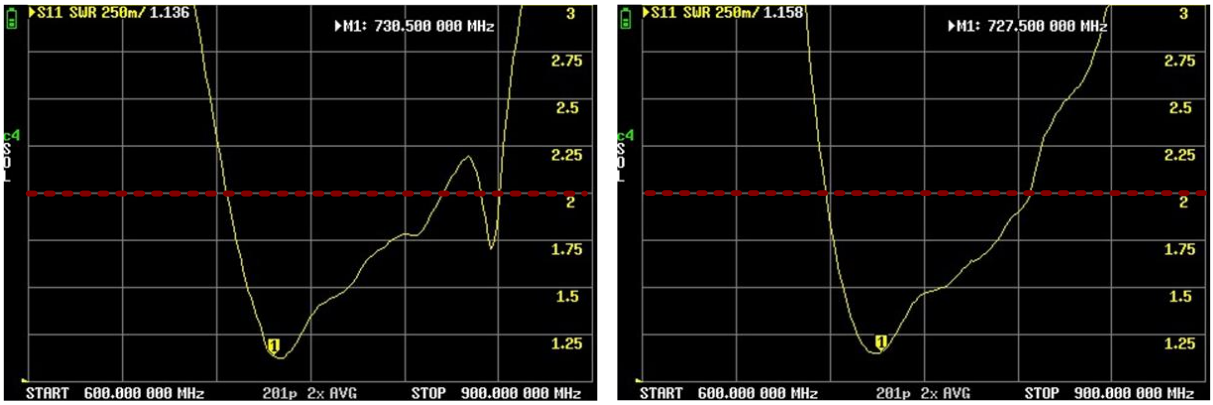

a *b*

Fig.22. Measured dependences of the VSWR of the collinear antennas on the frequency: *a* – with using the inductor; *b* – with using the quarter-wave stub

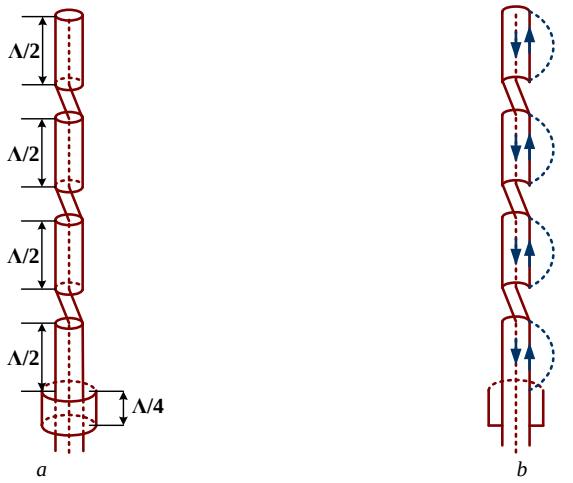

a *b*

Fig.23. Structure of the coaxial collinear antenna

The coaxial collinear antenna (Fig. 24) was designed and tested for the frequency band 5.5–5.8 GHz. For construction were used:

- microwave coaxial cable RG-402 (central conductor 0.92 mm, braid 3.58 mm; shortening factor 1.43);
- SMA connector series S-111.

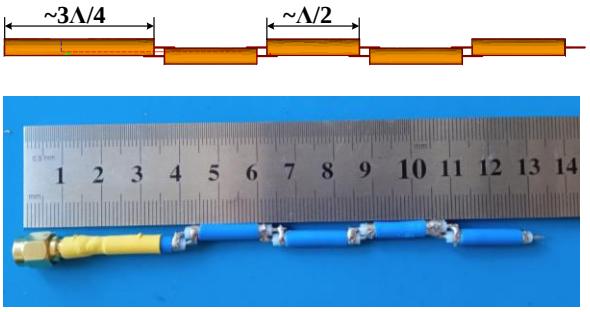

Fig.24. The coaxial collinear antenna

The main results of modeling and research of the coaxial collinear antenna are presented in Fig. 25-29.

Experimental study showed that the antenna operating frequency band reaches more than 300 MHz with VSWR < 2. The experimentally obtained frequency band is almost three times larger than that obtained in the simulation. This is due to the physical characteristics of the coaxial cable used for construction, since it is impossible to fully take them into account during modeling. The simulated gain reaches 5.5 dBi with the HPBW about 23 deg.

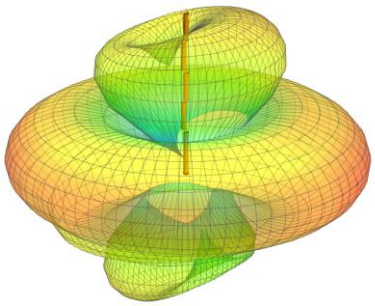

Fig.25. 3D radiation patterns of the coaxial collinear antenna

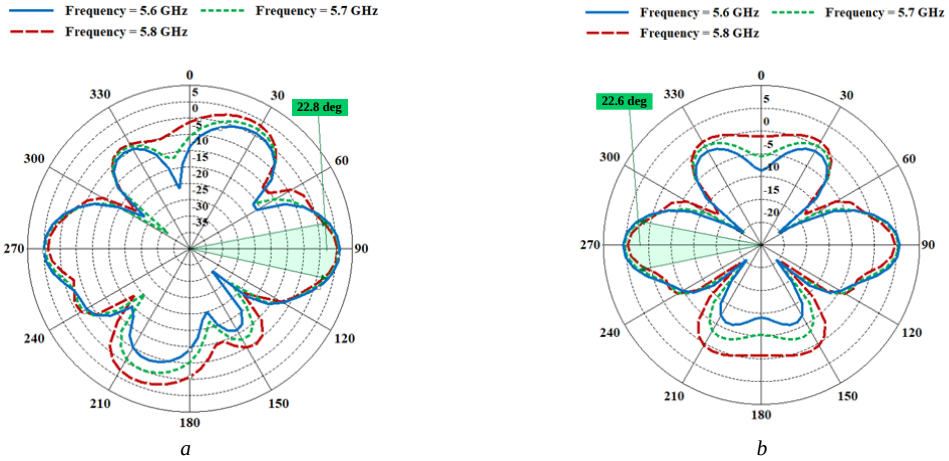

Fig.26. Radiation patterns of the coaxial collinear antenna: *a* – in the plane φ = 0 deg.; *b* – in the plane φ = 90 deg

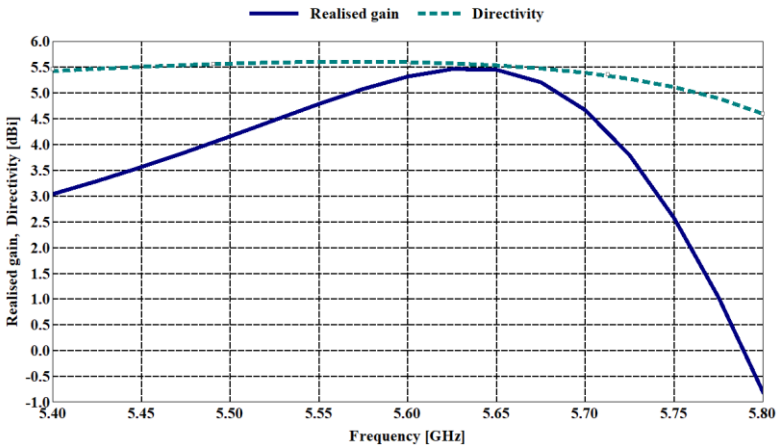

Fig.27. Dependences of the gain and the directivity of the coaxial collinear antennas on the frequency

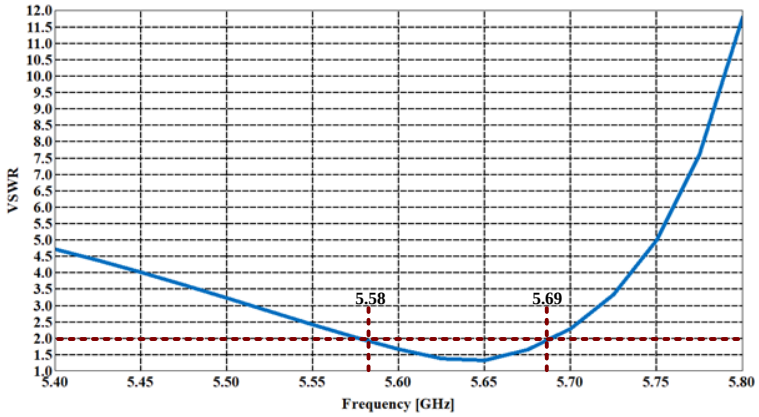

Fig.28. Dependence of the VSWR of the coaxial collinear antennas on the frequency

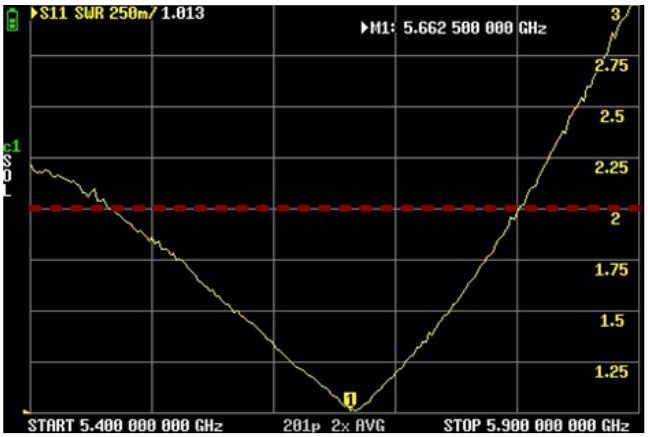

Fig.29. Measured dependences of the VSWR of the coaxial collinear antennas on the frequency

The following features were noted during the modeling and study of the experimental sample:

- the lengths of the coaxial cable sections must be shortened in comparison with the calculated ones to take into account the influence of the relative permittivity of the cable (shortening factor);
- when using the SMA connector of the series S-111, the antenna matching with the standard 50 Ohm feeder has improved, since in the connector design the part for cable crimping can play the role of a counterweight;
- it is possible to expand the operating frequency band through the use of coaxial elements of different lengths (the difference should be about 5–10%);
- radiation pattern asymmetry in planes at φ = 0 deg. and at φ = 90 deg. can be eliminated by improving the alignment of the coaxial antenna elements.

3.3. Yagi-Uda Antenna

The Yagi-Uda microstrip antenna belongs to the class of non-equidistant unequal-amplitude antennas with axial radiation. The operating frequency of 5.75 GHz was chosen for the study. To build the Yagi-Uda microstrip antenna (Fig.30), the dielectric substrate Roger RO4030 was used with the following parameters:

- relative permittivity 3.38;
- dielectric loss tangent 0.0027;
- substrate thickness 0.813 mm.

The main results of modeling and research of the Yagi-Uda microstrip antenna are presented in Fig. 31-35.

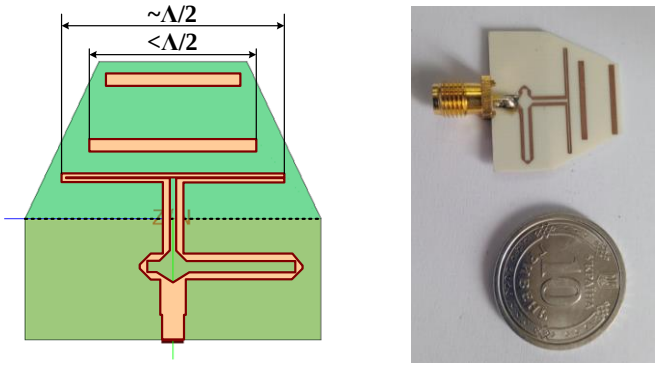

Fig.30. Yagi-Uda microstrip antenna

The experimental study showed that the operating frequency band reaches more than 400 MHz with VSWR < 2 and 200 MHz with VSWR < 1.5. The simulation obtained the gain of 4.8 dBi with the HPBW in the *E*-plane of about 74 deg. and in the *H*-plane of about 140 deg.

The following features were noted during the modeling and study of the experimental sample:

- the use of passive director microstrip dipole elements two to three times wider than the active dipole element can significantly expand the operating frequency band;
- increasing the number of passive director elements had almost no effect on the increase in the gain; therefore, there is no point in complicating the Uda-Yagi microstrip antenna design for these frequencies;

- the use of standard fiberglass laminate FR-4 to build an antenna at these frequencies leads to significant losses and, accordingly, a significant reduction in the gain.

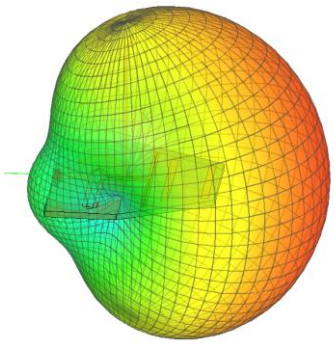

Fig.31. 3D radiation patterns of the Yagi-Uda microstrip antenna

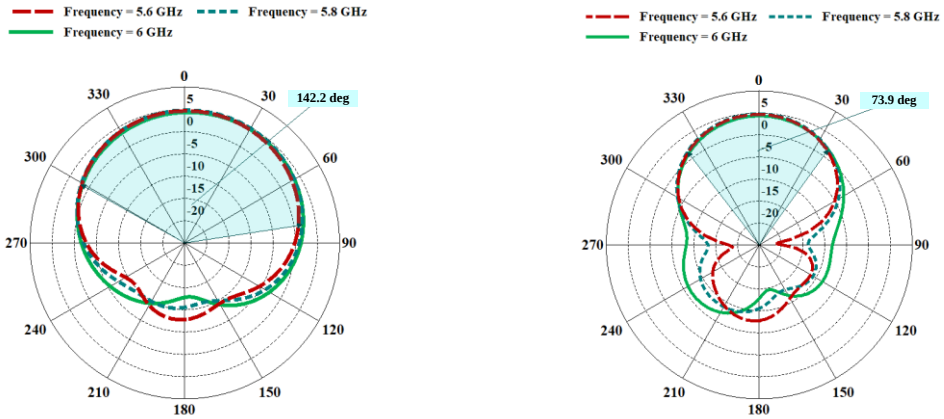

a *b*

Fig.32. Radiation patterns of the Yagi-Uda microstrip antenna: *a* – in the *H*-plane; *b* – in the *E*-plane

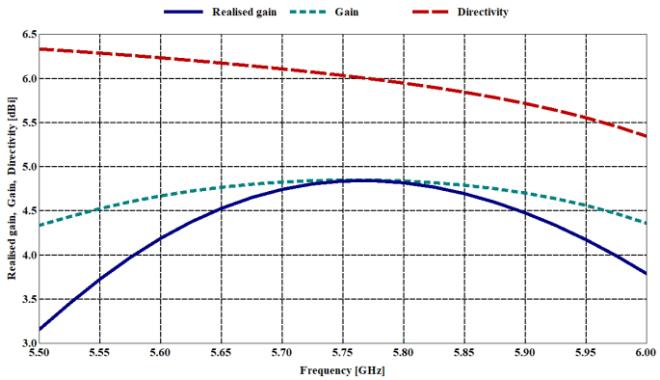

Fig.33. Dependences of the gain and the directivity of the Yagi-Uda microstrip antenna on the frequency

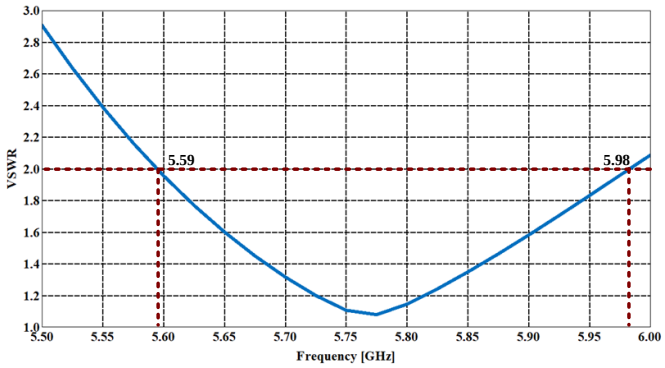

Fig.34. Dependence of the VSWR of the Yagi-Uda microstrip antenna on the frequency

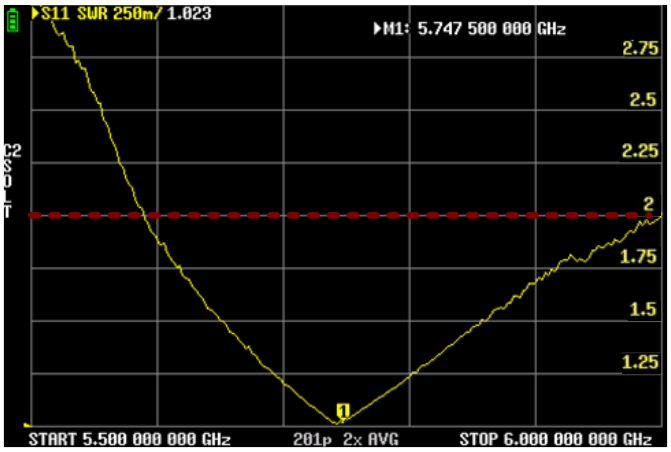

Fig.35. Measured dependences of the VSWR of the Yagi-Uda microstrip antenna on the frequency

3.4. Log-periodic Antenna

The log-periodic antenna (LPA), like the Yagi-Uda antenna, belongs to non-equidistant unequal-amplitude antennas with axial radiation. The process of microstrip LPA designing is described step by step in the work [6]. The symmetrical dipole elements of the LPA are fed by the strip two-wire feeder (Fig. 8).

The frequency range 2–6 GHz was chosen for the study. To build the microstrip LPA (Fig. 36), the dielectric substrate Roger RO4003C was used with the following parameters:

- relative permittivity 3.55;
- dielectric loss tangent 0.0021;
- substrate thickness 0.813 mm.

The main results of modeling and research of the microstrip LPA are presented in Fig. 37-41.

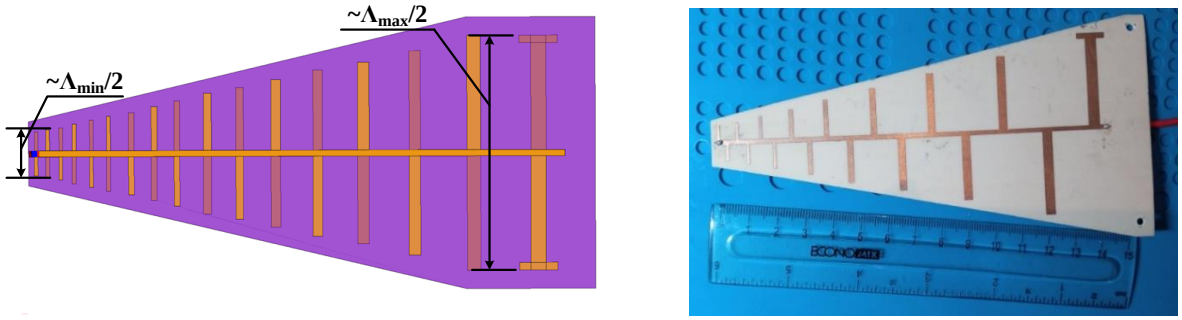

Fig.36. The microstrip LPA

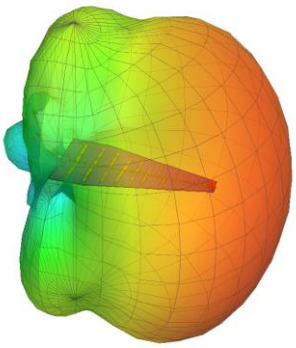

Fig.37. 3D radiation patterns of the microstrip LPA

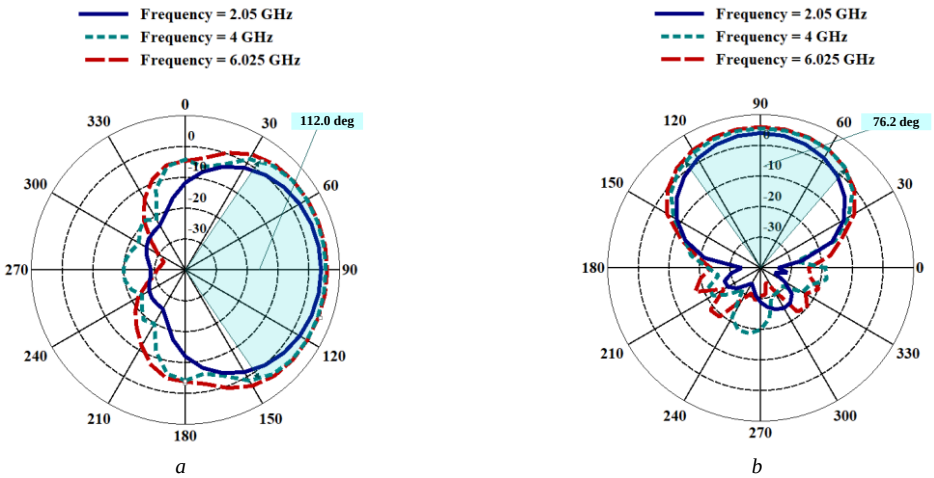

Fig.38. Radiation patterns of the microstrip LPA: *a* – in the *H*-plane; *b* – in the *E*-plane

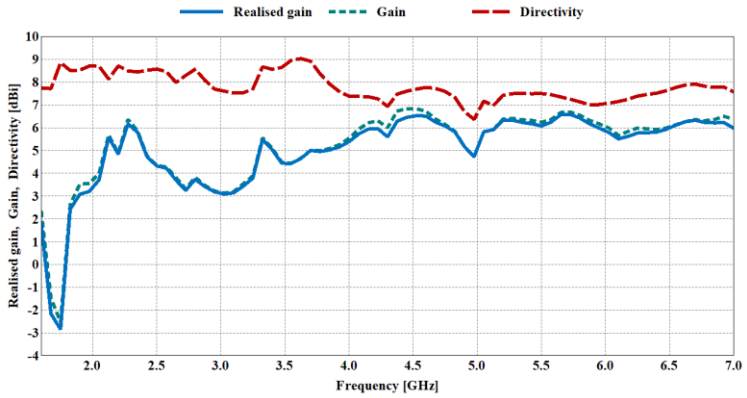

Fig.39. Dependences of the gain and the directivity of the microstrip LPA on the frequency

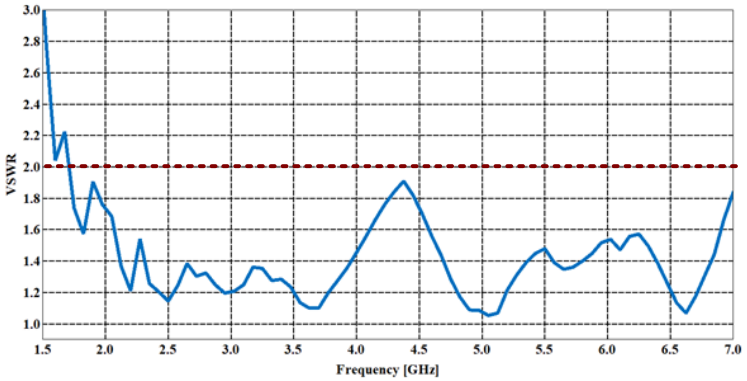

Fig.40. Dependence of the VSWR of the microstrip LPA on the frequency

The experimental study showed that the operating frequency band of the LPA reaches more than 4 GHz with VSWR < 2 (1.2–6.3 GHz). The simulation obtained the gain of about 6 dBi with the HPBW in the *E*-plane of about 76 deg. and in the *H*-plane of about 112 deg.

The following features were noted during the modeling and study of the experimental sample:

- for the manufacture of microstrip LPAs with the high overlap coefficient of the frequency range above 3 GHz, it is recommended to use special UHF substrates (for example, from Roger), since standard substrates for printed circuit boards do not guarantee the stability of their parameters in wide frequency range and introduce large losses;
- to increase the gain at the lower limit of the frequency range and to reduce the antenna dimensions, microstrip dipoles can be made in L-shaped (or T-shaped) form, which also allows optimizing the current distribution along the dipoles;
- the short-circuited section can be made with a bend, which significantly reduces the longitudinal antenna

dimension and has almost no effect on the radiation and matching characteristics;

- the short-circuited section can be replaced with an absorbing load (this is quite convenient for log-periodic antennas in microstrip design, when lightning protection is not a rigid obstacle, as in the case of wired antennas).

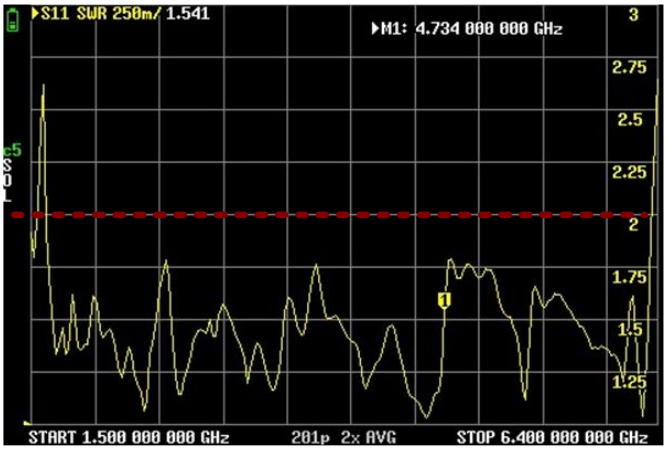

Fig.41. Measured dependences of the VSWR of the microstrip LPA on the frequency

4. Conclusions

This study has systematically explored the design, functionality, and optimization of passive antenna arrays for UAV communication systems. By integrating theoretical modeling with experimental validation, we have demonstrated how these arrays can significantly enhance signal reception and transmission capabilities in complex environments. The findings underscore the importance of passive arrays in improving the robustness and reliability of UAV communications, providing a foundation for future advancements in technology of antennas designed for UAVs. Recommendations are provided to guide further research and development, ensuring that UAV communication systems continue to evolve with increasing efficiency and effectiveness.

The theoretical justification, modeling, and experimental research of each type of AA has been performed and the features and recommendations that are useful both for beginners and professionals in the field of antenna design.

Antennas are one of the most important electronic devices in any UAV system because they allow the aircraft to transmit and receive information from other systems, including the ground control segment.

Antennas used both for the on-board segment and in mobile UAV control systems should be low-profile and compact, have a strong, simple and light design, and be easily mounted on surfaces of various shapes. The requirements for the radiation parameters of antenna systems, such as the gain factor and the shape of the directional pattern, can be significantly different depending on the purpose of the antenna.

The use of passive AAs makes it possible to form a specially shaped antenna pattern, control the antenna pattern and its orientation in space, as well as increase the radiation power. These AAs features significantly improve and expand the functionality of control, communications and surveillance systems. On the other hand, such antennas have a low price and do not require additional power sources.

This article has examined the main advantages of using AAs in the ground and airborne segments of the UAV system, discussed the basic principles of constructing passive AAs of various types: equidistant and non-equidistant, in-phase and phase-shifted, as well as the basic principles of designing AAs of the specified types. Modeling and experimental research of examples of AAs of different types of construction was carried out. Features of construction of various types of AAs are indicated, which can be applied in practice to ensure optimal results.

It has been shown that, when it is necessary transmit/receive an information signal with a gain factor greater than that of a classic dipole antenna, and without a specific reference to the azimuthal direction, it is advisable to use equidistant in-phase AAs both in the ground and in the on-board segments of the UAV system control. For example, it can be collinear antennas of different construction (wire or coaxial) depending on the required frequency and conditions of use. This allows the gain of up to 5 dBi with the HPBW of less than 30 deg. If it is necessary to transmit/receive signals in a specific sector of space, it is advisable to use directional AAs, for example, in-phase equidistant planar AAs with the number of elements depending on the required HPBW. This makes it possible to increase the gain by 12 dBi while reducing the HPBW, which can be less than 10 deg. depending on the number of AA elements. Such measures improve countermeasures against EW.

Directional antennas such as Yagi-Uda antenna and LPA have also been investigated. They have wider antenna pattern than equidistant in-phase flat AAs. For example, the microstrip Yagi-Uda antenna with two directors can have the gain of up to 5 dBi with the HPBW in the *E*-plane of about 76 deg. and in the *H*-plane nearly 112 deg. in the frequency band up to 400 MHz. If it is necessary to significantly expand the frequency band, it is advisable to use the LPA. For example, the microstrip 17-elements LPA can provide the gain of up to 6 dBi with the HPBW in the *E*-plane of about 80 deg. and in the *H*-plane about 120 deg.

Thus, in this work, modeling and research of samples of several types of passive AAs with static amplitude-phase distribution has been carried out. These samples refer to AAs, which are the most convenient for use in communication systems with UAVs because they satisfy the conditions of compactness, simplicity, reliability and have acceptable characteristics of radiation and coordination. After the theoretical justification, modeling and experimental study of the key features of each type of AAs, practical recommendations for the design of such antennas have been given.

References

[1] I. Jeon, S. Ham, J. Cheon, A. M. Klimkowska, H. Kim, K. Choi and I. Lee, "A Real-Time Drone Mapping Platform for Marine Surveillance," Int. Arch. Photogramm. Remote Sens. Spatial Inf. Sci., XLII-2/W13, 2019, pp. 385–391. https://doi.org/10.5194/isprs-archives-XLII-2-W13-385-2019.

[2] F. Abushakra, D. N. Elluru, A. K. Awasthi, S. Kolpuke, T. Luong, O. Reyhanigalangashi, D. Taylor and S. P. Gogineni, "A Miniaturized Ultra-Wideband Radar for UAV Remote Sensing Applications," National Oceanic and Atmospheric Administration, 2022. https://repository.library.noaa.gov/view/noaa/52285/noaa_52285_DS1.pdf.

[3] F. J. Yanovsky, H. W. J. Russchenberg and C. M. H. Unal, "Retrieval of information about turbulence in rain by using Doppler-polarimetric Radar," in IEEE Transactions on Microwave Theory and Techniques, Vol. 53, No. 2, 2005, pp. 444-450. https://doi.org/10.1109/TMTT.2004.840772.

[4] O. Spinka, S. Kroupa and Z. Hanzalek, "Control System for Unmanned Aerial Vehicles," 2007 5th IEEE International Conference on Industrial Informatics, Vienna, Austria, 2007, pp. 455-460. https://doi.org/10.1109/INDIN.2007.4384800.

[5] O. Sushchenko et al., "Design of Robust Control System for Inertially Stabilized Platforms of Ground Vehicles," IEEE EUROCON 2021 19th International Conference on Smart Technologies, Lviv, Ukraine, 2021, pp. 6-10. https://doi.org/10.1109/EUROCON52738.2021.9535612.

[6] A. Famili, A. Stavrou, H. Wang and J.-M. Park, "PILOT: High-Precision Indoor Localization for Autonomous Drones," in IEEE Transactions on Vehicular Technology, Vol. 72, No. 5, 2023, pp. 6445-6459. https://doi.org/10.1109/TVT.2022.3229628.

[7] Y. Averyanova, A. Rudiakova, and F. Yanovsky, "Aircraft Trajectories Correction using Sharing Operative Meteorological Radar Information," 2020 21st International Radar Symposium (IRS), 5-8 Oct. 2020, pp. 256 – 259. DOI: 10.23919/IRS48640.2020.9253799

[8] F. J. Yanovsky, "Evolution and Prospects of Airborne Weather Radar Functionality and Technology," 2005 18th Int. Conf. on Applied Electromagnetics and Communications, Dubrovnik, Croatia, 2005, pp. 1-4, doi: 10.1109/ICECOM.2005.204987

[9] R. B. Sinitsyn and F. J. Yanovsky, "MIMO radar copula ambiguity function," 2012 9th European Radar Conference, Amsterdam, Netherlands, 2012, pp. 146-149.

[10] A. Digulescu, C. Despina-Stoian, F. Popescu, D. Stanescu, D. Nastasiu and D. Sburlan, "UWB Sensing for UAV and Human Comparative Movement Characterization," Sensors, 23, 2023. https://doi.org/10.3390/s23041956.

[11] F. J. Yanovsky, V. E. Ivashchuk and V. P. Prokhorenko, "Through-the-wall surveillance technologies," 2012 6th International Conference on Ultrawideband and Ultrashort Impulse Signals, Sevastopol, Ukraine, 2012, pp. 30-33. https://doi.org/10.1109/UWBUSIS.2012.6379723.

[12] T. Fromenteze, C. Decroze and D. Carsenat, "UWB passive beamforming for large antenna arrays," 2014 IEEE International Conference on Ultra-WideBand (ICUWB), Paris, France, 2014, pp. 47-50. https://doi.org/10.1109/ICUWB.2014.6958949.

[13] P. Cheong, K. Wu, W. -W. Choi and K. -W. Tam, "Yagi–Uda Antenna for Multiband Radar Applications," in IEEE Antennas and Wireless Propagation Letters, Vol. 13, 2014, pp. 1065-1068. https://doi.org/10.1109/LAWP.2014.2328991.

[14] R. K. Tanti, S. Warathe and N. Anveshkumar, "Planar Yagi-Uda Antenna with Mirrored Ground Plane for WLAN," 2020 11th International Conference on Computing, Communication and Networking Technologies (ICCCNT), Kharagpur, India, 2020, pp. 1-5. https://doi.org/10.1109/ICCCNT49239.2020.9225278.

[15] Y.-H. Yang, J.-L. Guo, B.-H. Sun and Y.-H. Huang, "Dual-Band Slot Helix Antenna for Global Positioning Satellite Applications," in IEEE Transactions on Antennas and Propagation, Vol. 64, No. 12, 2016, pp. 5146-5152. https://doi.org/10.1109/TAP.2016.2623647.

[16] O. Shcherbyna, O. Tomai and O. Kozhokhina, "Quadrifilar Helical Antennas with Different Types of Supply Lines," 2018 Advances in Wireless and Optical Communications (RTUWO), Riga, Latvia, 2018, pp. 167-170. https://doi.org/10.1109/RTUWO.2018.8587877.

[17] O. Shcherbyna and O. Kozhokhina, "Construction principles of quadrifilar helical antenna," in Telecommunications and Radio Engineering, Vol. 79, No. 16, 2020, pp. 1441-1453. https://doi.org/10.1615/TelecomRadEng.v79.i16.30.

[18] O. Shcherbyna and R. Zadorozhniy, "The log-periodic dipole array antenna for monitoring," 2018 14th International Conference on Advanced Trends in Radioelecrtronics, Telecommunications and Computer Engineering (TCSET), Lviv-Slavske, Ukraine, 2018, pp. 583-586. https://doi.org/10.1109/TCSET.2018.8336270.

[19] K. Pojang and P. Rakluea, "The Design of Log Periodic Dipole Array Antenna for WLAN/LTE/UWB Applications," 2018 18th International Symposium on Communications and Information Technologies (ISCIT), Bangkok, Thailand, 2018, pp. 66-69. https://doi.org/10.1109/ISCIT.2018.8587918.

[20] M. A. K. S. Lubis, C. Apriono, F. Y. Zulkifli and E. T. Rahardjo, "Design of narrow wall slotted waveguide antenna for X-band application," 2017 Progress in Electromagnetics Research Symposium - Fall (PIERS - FALL), Singapore, 2017, pp. 2625-2628. https://doi.org/10.1109/PIERS-FALL.2017.8293579.

[21] M. R. Effendi, R. Ernanto and A. Munir, "4.2GHz compact collinear antenna for manpack satellite communication," 2018 International Workshop on Antenna Technology (iWAT), Nanjing, China, 2018, pp. 1-4. https://doi.org/10.1109/IWAT.2018.8379237.

[22] H. Sajjad, W. T. Sethi, K. Zeb and A. Mairaj, "Microstrip patch antenna array at 3.8 GHz for WiMax and UAV applications," 2014 International Workshop on Antenna Technology: Small Antennas, Novel EM Structures and Materials, and Applications (iWAT), Sydney, NSW, Australia, 2014, pp. 107-110. https://doi.org/10.1109/IWAT.2014.6958609.

[23] T.-Y. Chuang, W.-J. Liao, T.-G. Ma, Y. Lee and M.-C. Ho, "Compact directive array antenna design for UAV application," 2017 International Symposium on Antennas and Propagation (ISAP), Phuket, Thailand, 2017, pp. 1-2. https://doi.org/10.1109/ISANP.2017.8228780.
[24] P. M. Ruiz, X. Begaud, F. Magne, E. Leder and A. Khy, "Microstrip antenna array design for unmanned aerial vehicles detection radar," Advanced Electromagnetics, Vol. 12, No. 3, 2023, pp. 1-9. https://doi.org/10.7716/aem.v12i3.2066.
[25] C. A. Balanis, Antenna Theory: Analysis and Design. 4th Edition. New Jersey: John Wiley & Sons Inc., 2016.
[26] T. A. Milligan, Modern antenna design. New Jersey: John Wiley & Sons, Inc., 2005.

Authors' Profiles

Prof. Olga Shcherbyna, Professor at the National Aviation University, Kyiv, Ukraine. Her qualifications are as mentioned D.Sc. (Radio Engineering and Telecommunication Means), Ph.D. (Radio Engineering Devices and Television Systems), M.Sc. and B.Sc. (both in Radio Engineering) from the National Aviation University, Kyiv, Ukraine. She has 20 years of teaching experience and her areas of interest include antenna systems, microwave devices, electromagnetic compatibility. A total number of research publications is more than 120.

Oleksandr Zadorozhnyi, Associate Professor at the National Aviation University, Kyiv, Ukraine. His qualifications are Ph.D. (Radio-Engineering and Television Systems), M.Sc. and B.Sc. (Electronic Devices and Electronic Household equipment) from the National Aviation University, Kyiv, Ukraine. He has 10 years of teaching experience and his areas of interest include antenna systems, microwave devices, microcontroller technology. A total number of research publications is more than 20.

Olexii Stetsyshin, Student at the National Aviation University, Kyiv, Ukraine. His qualification is B.Sc. (Electronic) from the National Aviation University, Kyiv, Ukraine. At the moment he is studying at the National Aviation University to obtain master's qualification (Electronic Systems). His areas of interest include antenna devises, microwave devices, information security.

How to cite this paper: Olga Shcherbyna, Oleksandr Zadorozhnyi, Olexii Stetsyshin, "Passive Antenna Arrays in UAV Communication Systems", International Journal of Computer Network and Information Security(IJCNIS), Vol.16, No.4, pp.31-51, 2024. DOI:10.5815/ijcnis.2024.04.03